THE JOURNAL OF BIOLOGICAL CHEMISTRY
Vol. 279, No. 38, Issue of September 17, pp. 39829–39837, 2004
Printed in U.S.A.

Mapping of a Substrate Binding Site in the Protein Disulfide Isomerase-related Chaperone Wind Based on Protein Function and Crystal Structure*

Received for publication, June 18, 2004
Published, JBC Papers in Press, July 12, 2004, DOI 10.1074/jbc.M406839200

Kathrin Barnewitz‡, Chaoshe Guo‡, Madhumati Sevvana§, Qingjun Ma§¶, George M. Sheldrick§, Hans-Dieter Söling‡, and David M. Ferrari‡‖

From the ‡Department of Neurobiology, Max Planck Institute for Biophysical Chemistry, Am Fassberg 11 and the §Department of Structural Chemistry, University of Göttingen, Tammanstrasse 4, D-37077 Göttingen, Germany

The protein disulfide isomerase (PDI)-related protein Wind is essential in *Drosophila melanogaster*, and is required for correct targeting of Pipe, an essential Golgi transmembrane 2-*O*-sulfotransferase. Apart from a thioredoxin fold domain present in all PDI proteins, Wind also has a unique C-terminal D-domain found only in PDI-D proteins. Here, we show that Pipe processing requires dimeric Wind, which interacts directly with the soluble domain of Pipe *in vitro*, and we map an essential substrate binding site in Wind to the vicinity of an exposed cluster of tyrosines within the thioredoxin fold domain. *In vitro*, binding occurs to multiple sites within the Pipe polypeptide and shows specificity for two consecutive aromatic residues. A second site in Wind, formed by a cluster of residues within the D-domain, is likewise required for substrate processing. This domain, expressed separately, impairs Pipe processing by the full-length Wind protein, indicating competitive binding to substrate. Our data represent the most accurate map of a peptide binding site in a PDI-related protein available to date and directly show peptide specificity for a naturally occurring substrate.

PDI[1]-related proteins are residents of the lumen of the endoplasmic reticulum (ER) with various functions, including redox and chaperone activities, regulation of calcium homeostasis, and regulation of protein export from the ER for degradation. These functions are essential for maintaining a productive folding environment for many secretory proteins within the ER (1, 2) that may be critical for viability of the organism (3, 4). The chaperone function of these proteins, and probably to varying extents redox activity as well, relies on their ability to interact non-covalently with specific peptide sequences or epitopes in substrate proteins (2). However, until recently no concise data on peptide specificity, peptide binding sites, or the molecular basis for the observed substrate selectivity of these proteins were available. Data on such inherently weak interactions would require detailed knowledge of the three-dimensional structure of the protein concerned. Although independent NMR structures of the isolated a- and b-type thioredoxin fold domains (redox-active and redox-inactive domains, respectively) of PDI have been reported (5, 6), no complete structure of a eukaryotic PDI protein was available. Most PDI proteins are redox-active, and the involvement of relatively strong heteromeric disulfide bond formation and reduction in assays aimed at elucidating the nature of weak chaperone interactions poses further problems. Because the b′-domain has been identified as the major substrate binding site in PDI (7), much attention has been focused on these redox-inactive domains. However, the lack of suitable substrates of physiological relevance with a maturation process that can be readily monitored has complicated these studies. Thus much could be learned from the study of peptide binding and chaperone activity of a naturally occurring PDI family protein lacking redox properties but having a clearly defined substrate that can be studied both *in vivo* and *in vitro*.

We recently described the first crystal structure of a complete PDI-related protein of the eukaryotic ER (3). This protein, Wind, is essential in *Drosophila melanogaster* for dorsal-ventral patterning within the developing embryo, and it is required for ER export of an essential Golgi transmembrane proteoglycan modifying enzyme, Pipe (a 2-*O*-sulfotransferase) (8). Apart from a b-domain, Wind also has a unique C-terminal domain found only in the PDI-D subclass of PDI-related proteins (1). The function of the D-domain is poorly understood, although in *Dictyostelium discoideum* PDI-D it was shown to play a role in ER retention (9). Recently, we have shown that the Pipe-processing activity requires both the b- and D-domains of Wind. Although the mammalian Wind orthologue ERp28/29 cannot replace Wind in Pipe processing, the D-domains of both proteins could be exchanged, indicating functional conservation between the proteins (3).

Here, we show that Wind binds Pipe directly *in vitro*, and we map a putative peptide binding site within the Wind b-domain. We further describe a surface of the D-domain, the integrity of which is also required for Pipe processing. This work, based on the Wind crystal structure, represents the most accurate map of a peptide binding site within a PDI-related protein available to date and provides for the first time direct evidence for specific interaction with target sequences within natural substrates. The data presented suggest a solution to the apparent abundance and redundancy of PDI-related proteins within the ER lumen, indicating that discrete surface residues within and around a shallow pocket in the immediate vicinity of the CGHC

* This work was supported by Grants SO43/62-1, -2, and -3 and the Graduate College 60/3 of the Deutsche Forschungsgemeinschaft (to H.-D. S.). The costs of publication of this article were defrayed in part by the payment of page charges. This article must therefore be hereby marked "*advertisement*" in accordance with 18 U.S.C. Section 1734 solely to indicate this fact.

¶ Current address: EMBL Hamburg, Deutsches Elektronen-Synchrotron, Notkestrasse 85, D-22603 Hamburg, Germany.

‖ To whom correspondence should be addressed: Tel.: 49-551-201-1663; Fax: 49-551-201-1499; E-mail: dferrar@gwdg.de.

[1] The abbreviations used are: PDI, protein-disulfide isomerase; PDI-D, PDI-related protein containing a D-domain; ER, endoplasmic reticulum; GFP, green fluorescent protein; EGFP, enhanced GFP; GST, glutathione S-transferase; PBS, phosphate-buffered saline; DSS, disuccinimidyl suberate; BSA, bovine serum albumin.

redox-active motif of the a-domains or the corresponding residues of the b-domains determine substrate specificity for simple recognition motifs present in secretory proteins.

EXPERIMENTAL PROCEDURES

Cell Lines, Bacterial Strains, Plasmids, and Expression Vectors—Mammalian COS-7 and Vero cell lines were purchased from the European Collection of Animal Cell Cultures; XL1-Blue bacterial cells and the plasmid pBlueScript II were from Stratagene; pEGFP-N1 expression vector was from Clontech; and pQE-30 and pQE-60 expression vectors were from and Qiagen.

Antibodies—Antibodies against full-length *Drosophila* Wind were raised as described previously (3). Goat anti-rabbit Cy3-conjugated antibody was from Jackson ImmunoResearch.

Bacterial Expression Vector Constructs—Drosophila windbeutel full-length cDNA and Pipe cDNA were amplified and cloned as described (3). BamHI/SacI and NcoI/BglII PCR products encoding mature Wind were ligated into pQE-30 and pQE-60, respectively, generating constructs that have N-terminal (His-Wind) or C-terminal (Wind-His) His_6 tag extensions. The Wind mutant Wind-His Y55K and a construct encoding an N-terminally His_6-tagged D-domain (Wind-D, Ile^{150}-Leu^{257}) were made by standard mutagenesis techniques.

The sequence for the soluble, luminal domain of Pipe (Tyr^{40}-Asn^{403}) was ligated in frame via appended BamHI/EcoRI restriction sites 3′ to glutathione *S*-transferase within the vector pGEX-6P2 (Amersham Biosciences). This encoded a 69-kDa fusion protein (GST-Pipe) with an N-terminal GST moiety.

Mammalian Expression Vector Constructs—Full-length *windbeutel* was incorporated into the EcoRI/BamHI sites of pEGFP-N1, such that a stop codon preceded the enhanced green fluorescent protein (EGFP) sequence, ensuring translation of WT Wind alone (this construct is Wind*-EGFP-N1). Wind point mutants (Wind T23K, C24S, T25K, V28D,Y, C27S, D29N, D31N, E32K, R41S, D50A, D50N, D50S, I51S, I51R, A52S, Y53F, Y53S, Y55F, Y55K, Y55S, G56H, E57K, K58S, H59Y, E60A, E60Q, E60Y, T63K, K84D, K84N, K84S, D85N, Y86F, Y86L, Y86Q, Y86S, G87S, E88K, E88Q, E90R, D96N, D101N, D102N, K103S, P106D, D126N, C149S, R215A, R218D, L219S, and L232K), double (V28D/R41S, D31N/R41S, E90R/D29N, E90R/E60A, and L219S/E212Q), and triple (Y55K/D31N/R41S) mutants were constructed using appropriate primers and standard site-directed mutagenesis protocols, using Wind*-EGFP-N1 as template. Wind Y55K and D31N were described previously (3). Wind constructs with N-terminal extensions of 2 (GS, Wind+2), 4 (HHGS, +4), or 14 (ERMRGSHHHHHHGS, Wind+14) residues were created by insertion of a BamHI/AgeI fragment from the His-Wind construct into pEGFP-N1, followed by insertion via XhoI/BamHI sites of either of the three additional tags 3′ to the Wind signal sequence. A Wind construct (ss-D*) encoding the signal sequence appended to the Wind linker and D-domain (Ala^{138}-Leu^{257}) was created by insertion of a PCR fragment into the SacII/BamHI sites of pEGFP-N1, followed by insertion into XhoI/SacII sites of a synthetic oligonucleotide encoding the Wind signal sequence. Wind-N and Wind-N-KEEL, encoding the b-domain alone with or without an appended retrieval sequence respectively, were constructed as described (3). Pipe-GFP was constructed by ligating a KpnI/BamHI fragment of cloned Pipe into pEGFP-N1, generating full-length Pipe protein fused to the N terminus of EGFP.

Cell Culture and Immunofluorescence Assays—COS-7 and Vero cells were grown in 90% Dulbecco's modified Eagle's medium, 10% fetal bovine serum, with 2 mM L-glutamine and antibiotics, at 37 °C and 10% CO_2. For immunofluorescence labeling, cells transfected by electroporation were grown on coverslips overnight (17–20 h) then fixed with 4% paraformaldehyde. Bound Wind antibody, used at a 1:150 dilution, was detected with a 1:1000 dilution of goat anti-rabbit Cy3-conjugated antibody. Visualization of Cy3 and GFP was carried out on an Axiovert 200 microscope (Zeiss) with excitation filters of 565/30 and 480/40 nm, a dichroic beam splitter of 595 and 505 nm, and emission filters of 645/75 and 527/30 nm, respectively. Vero cells stably expressing WT Wind were created by selection of Wind*-EGFP-N1-transfected cells with 0.8 mg/ml G418 for 6 weeks. Isolated colonies were thereafter maintained in the presence of 0.4 mg/ml G418. MG132 proteasome inhibitor (Sigma) was applied to cells 12 h after transfection at 10 μM for 4 h.

Protein Expression and Purification—All proteins were expressed in *Escherichia coli* XL1-Blue by induction of A_{600} = 0.7 cultures for 3 h at 37 °C with 1 mM isopropyl-1-thio-β-D-galactopyranoside. Recombinant Wind proteins were harvested by sonication of lysozyme-treated cells in pH 8.0-adjusted phosphate-buffered saline, including 0.2 mM Pefabloc SC protease inhibitor, followed by addition of Triton X-100 to 0.1% (v/v) and application on a nickel-nitrilotriacetic acid nickel affinity column (Qiagen). Bound protein was washed and eluted according to the manufacturer's recommendations. Eluted protein was dialyzed against dialysis buffer (10 mM HEPES, pH 7.5, 50 mM NaCl, 0.01% (v/v) 2-mercaptoethanol), concentrated to 8–20 mg/ml, and stored at 4 °C. Protein purity was verified by SDS-PAGE and was consistently >95% for all proteins.

GST-tagged Pipe (GST-Pipe) was harvested by sonication of lysozyme-treated cells as above, followed by addition of 0.5 vol. of 60 mM EDTA, 6% (v/v) Triton X-100, 1.5 M NaCl. After 30-min incubation at 4 °C, pellets were collected by centrifugation at 20,000 × *g*, washed with 0.1 M Tris-Cl, pH 7.0, 20 mM EDTA, and collected again by centrifugation. Inclusion bodies were denatured with IB buffer (8 M urea, 25 mM Tris-Cl, pH 7.35, 50 mM dithiothreitol, 1 mM EDTA) for 2 h at 25 °C. The cleared 10,000 × *g* supernatant thereof was applied onto a (1 × 15 cm) Q-Sepharose column equilibrated with buffer IB. The pH of the flow through was set to 6.1 after dilution with 1 vol. of buffer B (8 M urea, 20 mM sodium phosphate, pH 6.1), applied onto a (1 × 3 cm) CM-Sepharose column, eluted with NaCl (0–0.5 M NaCl in buffer B), and stored at −20 °C.

In Vitro Cross-linking of Microsomal Protein—After overexpression of Pipe-GFP in COS-7 cells, crude microsomal preparations were made by disrupting PBS-washed cells by passage for 10 times each through 21-, 24-, and 27-gauge needles in KHM buffer (20 mM HEPES, pH 7.2, 110 mM potassium acetate, 2 mM magnesium acetate). After addition of protease inhibitor (Complete, Roche Applied Science), disuccinimidyl suberate (DSS) was added to 0, 0.25, 0.5, and 2 mM in Me_2SO. Controls were treated with similar amounts of Me_2SO alone. Samples were incubated for 30 min at room temperature, and reactions were stopped by addition of 20 mM glycine on ice for 15 min. Samples were precipitated with trichloroacetic acid and analyzed by immune blotting.

Direct Interaction of Wind with Pipe Protein—Recombinant GST-Pipe from inclusion bodies was spotted directly onto nitrocellulose membranes in increasing amounts, but in constant volumes. The membranes were blocked for 2 h with 5% non-fat milk powder in PBS then incubated overnight at 4 °C with either 5.6 μM Wind-His, 5.6 μM His-Wind, 1.7 μM Wind-His Y55K, or 5.6 μM Wind-D in 0.5% milk/PBS solution. After 1-h incubation each with Wind antibody and goat anti-rabbit horseradish peroxidase-coupled secondary antibody, with three intervening washes of 5 min each with 0.5% milk/PBS solution, the membranes were washed five times for 10 min with PBS/0.05% (v/v) Tween 20, and detected by chemiluminescence using the Western Lightning Chemiluminescence detection kit (PerkinElmer Life Sciences). Similar amounts of denatured BSA were used as control, and spots of Wind-His were added for calibration.

Direct Interaction of Wind with Pipe Peptides—To verify the nature of interacting peptides, 177 13-mers of Pipe, covalently bound to cellulose sheets (Jerini Peptide Technologies), were scanned. These peptides cover the luminal portion of Pipe, each consecutive peptide shifted by two residues toward the C terminus. The membrane was treated with 5% (w/v) nonfat milk powder in PBS for 2 h at room temperature, then incubated in 0.5% milk/PBS with either 5.6 μM Wind-His or 1.7 μM Wind-His Y55K, for 12 h at 4 °C. The sheet was washed three times for 5 min with 0.5% milk/PBS, then for 50 min with primary and secondary antibody as above. Bound protein was detected by chemiluminescence after five washes of 5 min each with 0.05% (v/v) Tween-20/PBS. The membrane was stripped according to the manufacturer's recommendations after detection of the Wind-His overlay, which preceded overlay with Y55K.

RESULTS

Direct Binding of Wind to Pipe—We have previously described a Wind mutant, Y55K, that cannot support ER export of Pipe (3). Further work[2] indicated that this mutant might have an increased affinity for Pipe substrate *in vivo*. In an attempt to visualize a direct interaction between Wind and Pipe, we overlaid membrane-bound spots of recombinant Pipe soluble domain (GST-Pipe) with recombinant C- or N-terminally His_6-tagged Wind (Wind-His or His-Wind, respectively), or the Wind-His Y55K mutant (Fig. 1*A*). The ensuing detection by chemiluminescence clearly shows an interaction of Wind

[2] K. Barnewitz, C. Guo, M. Sevvana, Q. Ma, G. M. Sheldrick, H.-D. Söling, and D. M. Ferrari, unpublished observations.

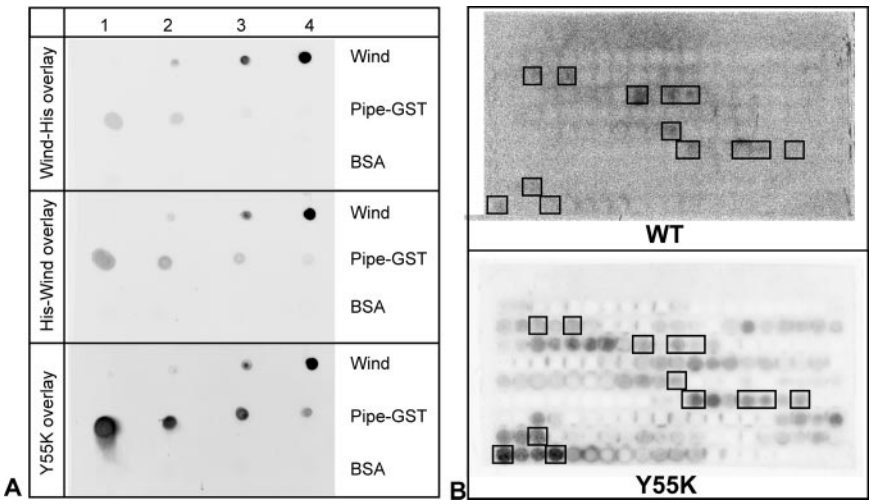

FIG. 1. **Direct binding of Wind to Pipe *in vitro*.** *A*, binding of Wind to denatured Pipe protein. Different amounts (0.2, 1, 4, and 16 μg from *right* to *left*) of GST-tagged Pipe (*Pipe-GST*), in 4 M guanidine hydrochloride, were spotted onto nitrocellulose. BSA, treated similarly was used as control. Wind was spotted for calibration (1, 5, 10, and 100 ng from *left* to *right*). The blots were overlaid with 5.6 μM Wind-His (*top panel*), 5.6 μM His-Wind (*middle panel*), or 1.7 μM Wind Y55K (*lower panel*) and detected using Wind antibodies. Pipe-GST, but not BSA, is recognized by all three proteins, with stronger binding to the Y55K mutant. *B*, binding of Wind to 13-mer Pipe peptides. The membrane was incubated with 5.6 μM Wind-His (*top panel*) or 1.7 μM Wind Y55K (*lower panel*). Peptide spots showing bound Wind, detected using Wind antibodies, are marked with *black boxes*, and corresponding spots on the Y55K blot are similarly marked. Binding to Wind-His was performed first. Detection times were 5 min for Wind and 2 min for Y55K.

and Pipe, detectable at amounts of Pipe as low as 10 pmol. Interestingly, the strength of interaction with Pipe was of the order Wind-His Y55K > His-Wind > Wind-His. This finding is consistent with independent experiments indicating that the Y55K mutant displays a dominant negative phenotype *in vivo* (see below). The fact that the N-terminally His_6-tagged Wind construct binds denatured substrate further indicates that peptide binding does not require surfaces within the dimer cleft, consistent with our further experimentation (see below). In contrast, no binding under these conditions was found for blots overlaid with the D-domain of Wind (data not shown), indicating that the D-domain either cannot bind substrate in the absence of the b-domain or that the target epitope is non-linear or offers binding kinetics too transient for visualization by the techniques employed here.

To narrow down the search further for candidate peptide sequence(s) in Pipe responsible for the interaction with Wind, cellulose-immobilized 13-mers of Pipe were scanned with Wind or Wind Y55K. Similar approaches have been used for investigating peptide binding to chaperones such as DnaK and Hsc66 (10, 11). Here, the detection pattern of protein-bound spots for both applied proteins was similar, although the Y55K mutant bound much stronger and also detected more spots (Fig. 1*B*). Several non-overlapping sets of peptides were detected (Fig. 1*B* and Table I) indicating that multiple Wind binding sites may exist in Pipe. Analysis of these sequences shows great variation in sequence and character, with the notable exception of a core of two consecutive, preferentially Phe or Tyr aromatic residues, although the Y55K mutant allows other hydrophobic residues as well (Table I). Importantly, all five peptide sequences that bind Wind are also recognized by, and bind with higher affinity to, the Y55K mutant. Of these sequences, the four that bind strongest to the Y55K mutant all contain the diaromatic motif, consisting of Phe or Tyr residues, with the fifth sequence possibly with the recognition motif Y*X*Y (where *X* is Gln) or YL. Barring potential pitfalls such as accessibility and peptide conformation, a tentative ranking of these residues in terms of their binding affinity to the Y55K mutant gives the order: FY > FF > YF > Y*X*Y (or YL).

The Thioredoxin Domain Has a Distinct Peptide Binding Site Close to the Dimer Cleft—We have previously shown that the

TABLE I

Wind Y55K binding peptides in order of binding affinity

Peptides that bind both Y55K and C-terminally tagged Wind (Wind-His) are shown in boldface. Both proteins preferentially bind peptides that contain an aromatic core of two Phe or Tyr residues (underlined), although at least Y55K also binds peptides with a single aromatic residue juxtaposed to a large hydrophobic amino acid.

	Peptide sequence	Pipe residues
1.	**VRRNFTNEIEFYQFCRQRL**HKQY	Val359-Tyr381
2.	NTTLSVLEKYVP**RFFEGVRDIYATS**	Asn311-Ser335
3.	MELLRRLSERNNFQF	Met129-Phe143
4.	FNRVPKVGSQTFMELLRRLSERN	Phe117-Asn139
5.	**VEGIGDHRRQSLFFCGHDYECTPFN**	Val261-Asn285
6.	YVRAPW**YFVERKAAFPDLPLP**	Tyr213-Pro233
7.	SVFIKHVCFTNFTKFNLPRPIYLNVVR	Ser175-Arg201
8.	QFCRQRLHKQYLAAHLPQRIITD	Gln371-Asp393
9.	PFNTVGALERAKF	Pro283-Phe295
10.	DINT**LHGTYQYLKSTGQMSSL**NV	Asp79-Leu99
11.	NNTRKAQMELVFFNRVPKVGSQT	Asn105-Thr127

b-domain of Wind contains a patch around Tyr^{55} that is required for Pipe processing (3). To define the residues involved in greater detail, we employed site-directed mutagenesis techniques to exchange 30 surface-exposed residues within 20 Å of Tyr^{55}. These mutants were then tested for their ability to process Pipe, evaluated by the translocation of Pipe from the ER to the Golgi. Of these mutants, six (D50A, Y53S, E60Q, Y86Q, K84D, and P106D) were found in addition to the one reported previously (Y55K) (3) that completely abrogated Pipe processing (Fig. 2). Of the residues concerned, all but Lys^{84} are conserved in mammalian Wind orthologues.

Excluding Glu^{60} (see below), the Cα atoms of these residues define a roughly elliptical area of ~180 $Å^2$ with no residue, apart from Pro^{106}, more than 10 Å distant from the center, that may constitute all or part of the substrate binding site of Wind

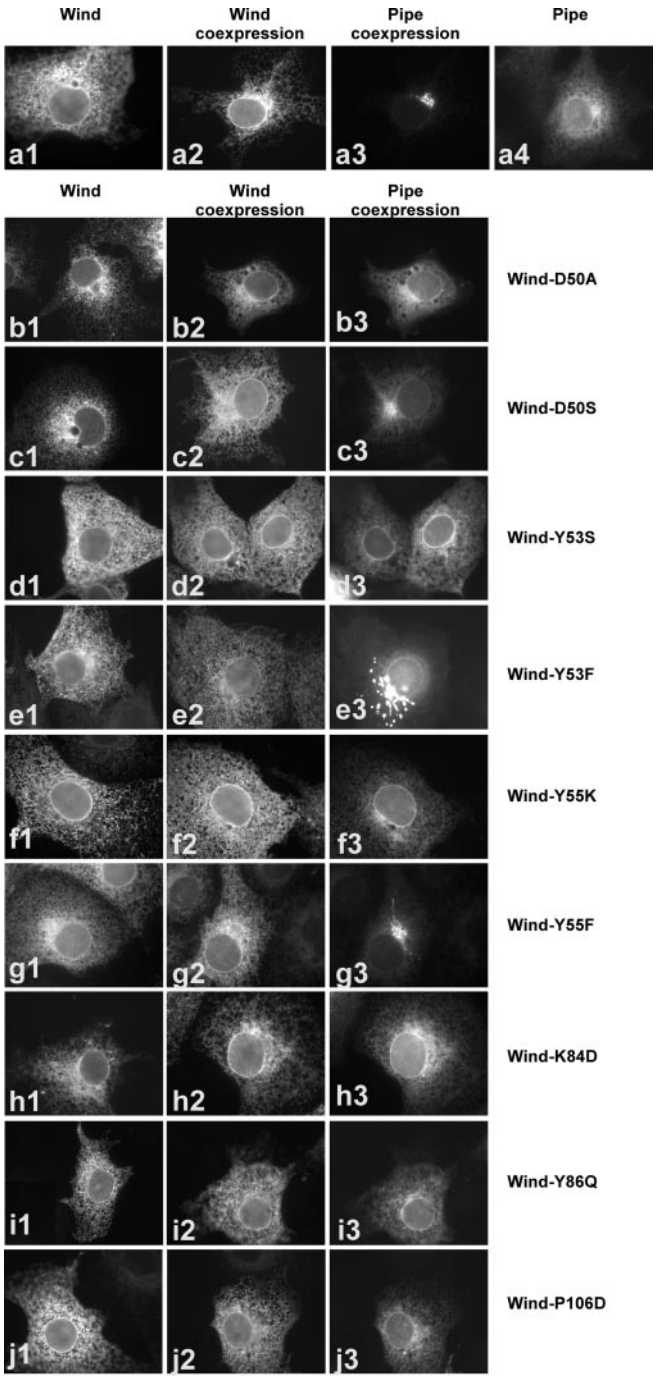

FIG. 2. **Effect of Wind mutants on Pipe export to the Golgi in COS cells.** The *first column* shows expression of WT Wind or the indicated Wind mutant alone, whereas the *second* and *third columns* show co-expressing cells with Wind and Pipe-GFP, respectively. Whereas ER-localized Pipe-GFP (*a4*) is re-routed to the Golgi (*a3*) in cells co-expressing WT Wind, in cells expressing Wind mutants of the Tyr^{55}-proximal pocket show severe (D50A (*b3*) and P106D (*j3*)) or partial (D50S (*c3*)) impaired Pipe processing. Mutation of a residue of the tyrosine cluster significantly (Y53S (*d3*) and Y55K (*f3*)) reduced Pipe transport, unless replacement is by Phe, in which case export proceeded normally (*e3* and *g3*). Mutation of residues in the PDI-Dβ loop can also prevent Pipe export (K84D (*h3*) and Y86Q (*i3*)).

(see Fig. 10 below). The three tyrosines, Tyr^{53}, Tyr^{55}, and Tyr^{86} form a loose cluster with the inner Tyr^{53} and Tyr^{55} at the position of Trp^{52} and Cys^{56} of the *WCGHC* motif of the PDI a-domain and the outer Tyr^{86} within the unique, inserted loop between β3 and α3 (hereafter termed the PDI-Dβ loop), more distal to the dimer interface.

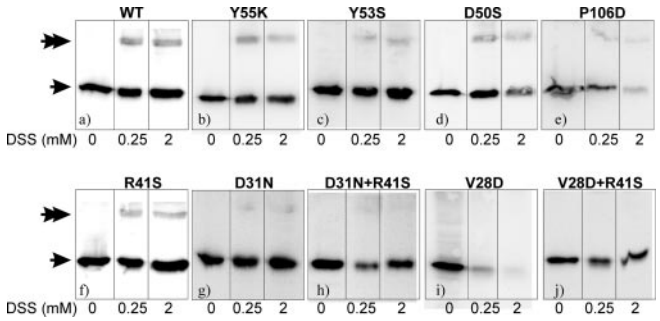

FIG. 3. **Effect of mutations on the dimerization and aggregation of Wind.** Cross-linking of extracts from COS cells expressing WT Wind (*a*), Y55K (*b*), Y53S (*c*), D50S (*d*), or R41S (*f*) with 0, 0.25, or 2 mM DSS shows the Wind dimer (*double arrow*) at roughly unaltered ratios to monomer (*single arrow*) for all species. In all cases, monomer and dimer are visible up to 2 mM DSS, indicating solubility of the proteins. P106D (*e*) shows reduced solubility, although some monomer and dimer are still visible. The V28D mutation prevents dimerization but causes complete aggregation of the monomeric protein (*i*), although this can be fully stabilized by incorporation of the R41S mutation (*j*). The small amount of the D31N dimer (*g*) is sufficient to allow for Pipe processing. Incorporation of the R41S mutation efficiently prevents dimer formation (*h*) and abrogates Pipe transport. In contrast, the R41S mutation alone is not sufficient for disrupting Wind dimerization (*f*).

Asp^{50} Is Located in a Pocket Near Tyr^{53} and Is Essential for Pipe Processing—We initially found that mutation of Asp^{50}, a conserved residue in all PDI-Dβ proteins, to Asn (D50N, data not shown) completely abrogated Pipe processing. Replacement of Asp^{50} with Ser allowed some retention of function, resulting in partial Golgi localization of Pipe (Fig. 2, *panels c1–c3*) in some cells, whereas replacement with Ala led to complete loss of activity (Fig. 2, *panels b1–b3*) similar to D50N. Protein expression, localization, and dimerization of D50A and D50S seem normal in our assays (Fig. 2, *panels b1–b3* and *c1–c3*, and Fig. 3, *panel d*). Asp^{50} is located at the bottom of a shallow pocket flanked to one side by hydrophobic atoms and Tyr^{55}, with the conserved Pro^{106} to the other side (see Fig. 10). Pro^{106} is a conserved *cis*-proline found also in the a-domain of PDI, but it is absent from the b-domains. It has been suggested that this proline may form part of a hydrophobic substrate binding site in other thioredoxin-related proteins (12).

Most Wind Mutants Display Normal Expression and Dimerization Levels, Indicating Normal Folding in the ER—We can exclude the possibility that the D50A and tyrosine mutations have significantly destabilized the Wind dimer or prevented dimerization as cross-linking of microsomal proteins *in vitro* clearly showed the presence of the wind dimer at a roughly unaltered ratio to monomer (Fig. 3), and they do not display obvious aggregation in contrast to Wind V28D (see below). For Pro^{106}, the situation is more complex. We have indicated earlier that the structure of the b-domain of Wind is intermediary between that of the a- and b-domains of PDI (3). Similar to the corresponding proline in the PDI a-domain, the partially exposed Pro^{106} assumes a *cis* conformation in the Wind b-domain. However, the corresponding proline in the rat orthologue ERp29 was shown to be in *trans* conformation (13). In the PDI b-domain, the corresponding residue is Asp^{201} (*trans*). The thioredoxin fold nevertheless does not show large structural variation around this residue. Thus our P106D mutation need not necessarily disrupt the thioredoxin fold significantly. Indeed, as shown in Figs. 2 and 3, expression levels, localization, and the dimer to monomer ratio appear normal for this mutant, despite some aggregation, although more rigorous approaches would be necessary to prove this point. Additionally, we have already shown that recombinant Y55K has normal chromatographic behavior when compared with WT (3) and that the crystal structure of the Y53S mutant shows no significant

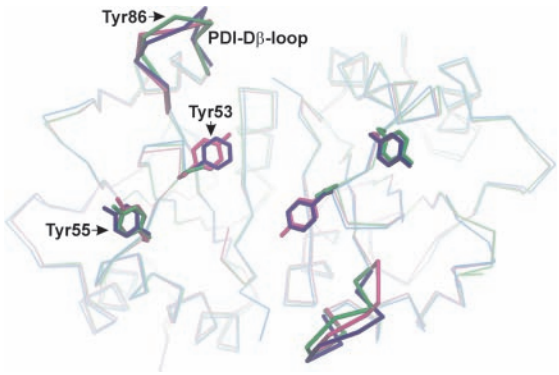

FIG. 4. **Mutation of Tyr^{53} does not result in significant structural changes in Wind.** Superimposed structures of the b-domains of Y53S (*green*), Y53F (*blue*), and wild-type (*purple*) show no significant structural changes in the backbones of either protein. The change visible in the PDI-Dβ loop is within the range observed for the loops of both monomers of the wild-type protein (for details see M. Sevvana, G. Chaoshe, H. D. Söling, G. M. Sheldrick, and D. M. Ferrari, manuscript in preparation). Fig. produced with DINO (available at www.dino3d.org).

structural changes compared with that of the His-Wind protein[2] (Fig. 4).

The PDI-Dβ Loop Plays No Essential Role in the Processing of Pipe—Lys^{84} is in the partially conserved PDI-Dβ loop (^{84}KDYGEL^{89}) between strand β3 and helix α3 (see Fig. 4). This loop does not originate from the thioredoxin domain, but the β3/α3 turn is also exploited in other thioredoxin-related proteins for non-related inserts of varying size and structure (14, 15). In these proteins it has been suggested that the insertion may play a role in substrate binding (14). In Wind, the PDI-Dβ loop is <6 Å from Tyr^{53} and ~10 Å from Tyr^{55}.

Initially, we found that exchange of Lys^{84} with Asp (K84D) or Tyr^{86} with Glu or Leu (Y86Q and Y86L), respectively, resulted in a complete loss of Pipe-processing activity (Fig. 2). However, further replacements (K84S, K84N, Y86S, and Y86F) had no significant effect on Pipe processing. The likely effect of both the K84D and Y86Q phenotypes was therefore more probably due to another, indirect effect. Furthermore, we could replace other residues in the loop (D85N, G87S, or E88K) with no effect on Pipe export (data not shown). Thus we conclude that, for Pipe processing, no essential interaction is required with specific residues within the PDI-Dβ loop.

It Is Primarily the Aromatic/Hydrophobic Nature of the Tyrosine Cluster That Is Essential, Not the Polar Character—To investigate the nature of the requirement of the tyrosine cluster residues, we created mutants with one of the three tyrosines replaced with phenylalanines. None of these mutants had any negative effect on Pipe processing, whereas other single mutants at these sites (Y53S, Y55K, Y55S, Y86Q, and Y86L) completely abrogated the processing of Pipe in most cells (Fig. 2). Interestingly, however, although both Y53S and Y55S are functionally inactive, the Y86S mutant retains processing activity. This indicates that the inner Tyr$^{53/55}$ pair within the cluster provides an aromatic/hydrophobic surface essential for Pipe processing, whereas the role of the outer Tyr^{86} in the PDI-Dβ loop seems dispensable for this substrate.

Mutations in the Tyrosine Cluster Enhance Substrate Binding but Reduce Processing Efficiency of Pipe—Interestingly, we noticed that co-expression of either Wind Y53S, Y55K, K84D, or Y86Q and Pipe in COS cells caused a concomitant decrease in levels of both the Wind mutant and Pipe, which was not observed when the WT protein was used. In the case of Y53S and K84D, protein levels rose again to near-normal in the presence of the proteasome inhibitor MG132 (Fig. 5). We therefore wished to know whether the mutations led to concomitant co-degradation of both species either due to reduced dissociation or malfolding of the associated proteins. For this purpose, we constructed a stable Vero cell line expressing wild-type Wind by selection for G418-resistance of cells transfected with the Wind*-EGFP-N1 construct.

Transfection of these cells with Pipe-GFP led to accumulation of the protein in the Golgi, as expected (Fig. 6). However, when the cells were co-transfected with Pipe and either Wind Y53S, Y55K, or Y86Q, Pipe failed to leave the ER in a majority (50–60%) of cells. Similar results were obtained with the K84D mutant (Fig. 6). In contrast, using the R215A D-domain mutant (see below) that, when expressed with Pipe alone, is unable to support Pipe export from the ER, no decrease in Pipe targeting was observed in the stably transfected cells (Fig. 6). These results indicate that the tyrosine mutants function as dominant negative mutants by sequestering Pipe away from WT Wind, either by catalyzing an irreversible off reaction, and/or by more stably associating with Pipe.

Taken together with the results from our *in vitro* denatured substrate and peptide binding assays (above), our data indicate that the Wind tyrosine mutants associate more stably with Pipe than does the wild-type protein. This association is so stable that both chaperone and substrate seem to undergo selective, simultaneous degradation possibly by being recognized as a malfolded complex.[3] In contrast to the tyrosine cluster residues, neither of the intercalated hydrophobic residues, Ile^{51} and Ala^{52}, are essential for Pipe processing as indicated by an unimpaired Pipe transport by the Wind mutants I51S, I51R, and A52S (data not shown).

Neither the Charged Nature of the Dimer Cleft, nor the Space within It, Are Essential for Pipe Processing—In Wind, dimerization leads to formation of a negatively charged cleft that is large enough to partially accommodate an extended polypeptide (3). Each subunit provides five acidic residues, three of which are conserved, with an additional contribution by Glu^{32} near the entrance to the cleft. We created a range of mutants each with either one or two acidic residues exchanged (D29N, D31N, E32K, E60Q, E88Q, E88K, E90R, E90R/D29N, and E90R/E60A). Of these mutants, only E60Q, which is within 8 Å of Tyr^{55}, had a negative impact on Pipe processing (data not shown), with a complete loss of Pipe export from the ER. However, an exchange of Glu^{60} with a small, hydrophobic residue (E60A) or with a bulky, polar one (E60Y) had no adverse effect on ER export of Pipe, indicating that the E60Q effect was unlikely due to be the requirement by substrate for interaction with a specific residue at this position.

We also constructed additional Wind mutants, in each of which one residue within the cleft was replaced with either a residue of different character or opposite charge (C24S, T25K, C27S, D29N, K58S, H59Y, T63K, E88K, and E88Q). None of these mutations, located throughout the cleft, interfered with Pipe processing (data not shown). We conclude that no specific interactions with the side chains of residues in the cleft are required for processing of Pipe.

To investigate whether access to the space in general throughout the cleft was important for substrate interactions, we constructed mutants of Wind with two, four, or fourteen extra residues appended to the N terminus of the mature sequence (Wind+2, +4, and +14). The N terminus is near the middle of the cleft, halfway from the cleft floor (3). The three constructs introduce additional residues within the cleft, thus obstructing access to it. In addition, the Wind+14 construct was expected to extend above the top face of the dimer and thus

[3] K. Barnewitz, C. Guo, M. Sevvana, Q. Ma, G. M. Sheldrick, H.-D. Söling, and D. M. Ferrari, manuscript in preparation.

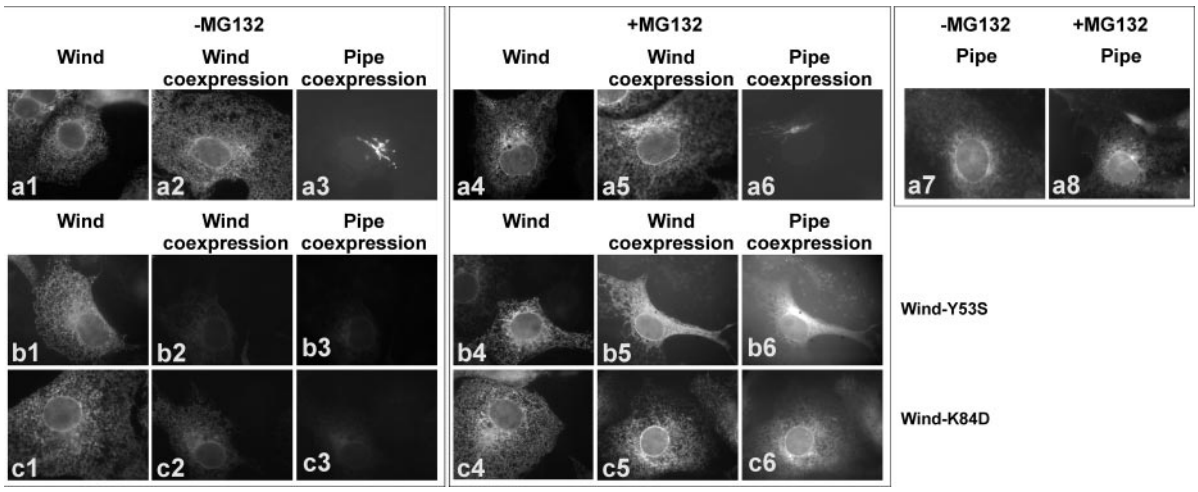

FIG. 5. **Stabilized substrate binding of the Wind mutants Y53S and K84D during co-expression with Pipe leads to co-degradation of both chaperone and substrate in COS cells.** During co-expression with Pipe, WT Wind levels in the ER do not change significantly when compared with cells expressing Wind alone (*a1* and *a2*), nor do they change in the presence of the proteasome inhibitor MG132 (*a4* and *a5*). The inhibitor itself has no effect on the Wind activity, allowing normal Golgi transport of Pipe (*a3* and *a6*). Although levels of Pipe are relatively stable in the presence of MG132 (*a7* and *a8*), levels of both Wind Y53S and Pipe decrease greatly during co-expression (*b2* and *b3*). The same observation applies for Wind K84D (*c2* and *c3*). In contrast, levels of either mutant remain constant independently of MG132 when expressed alone (*b1*, *c1*, *b4*, and *c4*). For both mutants, Wind and Pipe protein levels remain constant in the presence of inhibitor (*b5*, *b6*, *c5*, and *c6*). Compared images have undergone identical post-processing.

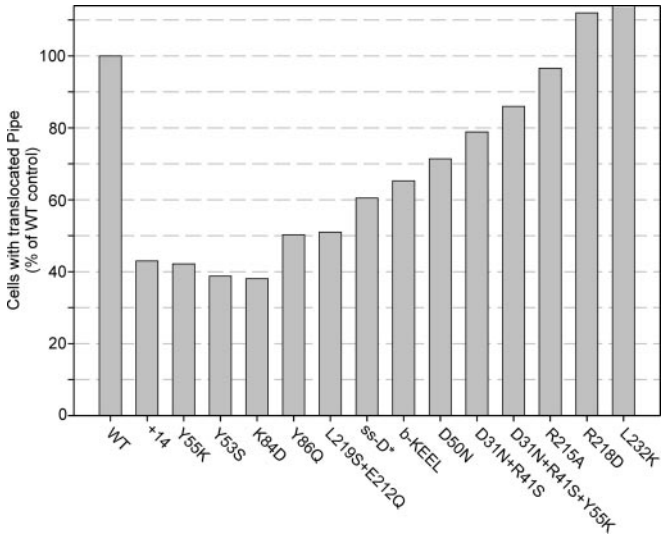

FIG. 6. **Pipe processing efficiency in Vero cells stably expressing Wind varies for cells co-expressing different Wind mutants.** Data reflect the number of cells in which Golgi staining was clearly seen. Mean values from 400 cells are expressed as percentage of the normalized value obtained for WT Wind. Note that the real effects of the mutations are likely to be greater as co-transfection efficiencies were normally less than 50%.

possibly prevent access of a bulky protein to the tyrosine cluster. Interestingly, although neither Wind+2 nor Wind+4 showed any effect on Pipe processing, the Wind+14 construct completely abrogated Pipe export from the ER (Fig. 7). It is noteworthy, however, that the *E. coli* His-Wind construct, which is similar to the Wind+14 construct used in COS cells, can nevertheless bind denatured substrate *in vitro* (Fig. 1*A*). This indicates that 1) the space within the dimer cleft is not essential for substrate processing and 2) unimpeded access to the surface tyrosine cluster is required for Pipe processing *in vivo*.

The D-domain Competes in Vivo for Binding to, but Cannot Process, Pipe—The Wind D-domain can be functionally replaced by the D-domain of mouse ERp29 (3). Although we observed no binding by the D-domain to denatured Pipe spots, it was nevertheless possible that a second, albeit weak, binding site might exist in this domain. If this were the case, and because the D-domain does not otherwise interact with the b-domain (based on the crystal structure and *in vitro* results, data not shown), one might expect that the D-domain could compete for substrate binding when expressed *in vivo* together with full-length Wind.

We therefore transfected Vero cells stably expressing Wind with both Pipe-GFP and the Wind D-domain (ss-D*), using Wind+14 (which corresponds to a dimeric Wind protein with inactivated b-domains) and the Wind+4 construct as controls. A significant decrease in Pipe transport was observed in cells expressing the ss-D* or Wind+14 constructs (decrease of 40 and 57%, respectively, Fig. 6) but not in the case of co-expression with Wind+4 (data not shown). Because the real effect of the mutants is likely to be much higher (co-transfection efficiency was normally in the range of 50%) these results show that the D-domain might contain a discrete site for interaction with Pipe, which is able to compete with full-length Wind for binding to substrate. The Wind+14 construct prevents ER export of Pipe, probably by preventing interaction of substrate with the tyrosine cluster as suggested above, whereas the N-terminal extension of Wind+4 is too short to interfere with Pipe binding.

We then created several single D-domain mutants in which conserved residues were exchanged and examined their ability to process Pipe. Three of these mutants, R215A, R218D, and L232K, as well as the double mutant L219S/E212Q, significantly or completely inhibited Pipe processing (Fig. 8). These residues form a cluster at the end of α8 and the N terminus of α9. Although none of the single point mutants R215A, R218D, or L232K had any adverse effect on Pipe processing when expressed in our stably transfected Vero cell line (Fig. 6), co-expression of the L219S/E212Q double mutant led to a significant decrease (50%) in Pipe export. Because expression of the D-domain (ss-D*) also reduces Pipe processing efficiency, and because the b-domain alone cannot process Pipe (Fig. 6) (3), our data suggest that the D-domain may provide a distinct site required for substrate interaction.

Dimerization of Wind Is Required for Productive Pipe Binding and Processing—We reported previously that the Wind

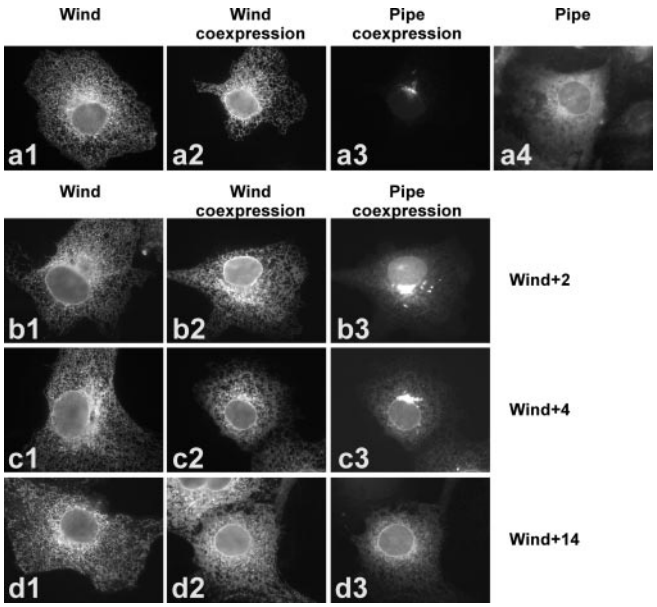

FIG. 7. **Access to the tyrosine cluster is essential for Pipe processing.** Wind mutants with N-terminal extensions of 2 (*b3*) or 4 (*c3*) residues allow normal Pipe processing, but export is blocked by extension with 14 residues (*d3*). All mutants are similarly expressed in the ER (*b1*, *c1*, and *d1*) when compared with wild type (*a1*) and are present in co-transfected cells (*b2*, *c2*, and *d2*). The ER-retained distribution of Pipe when expressed alone is shown in *a4*.

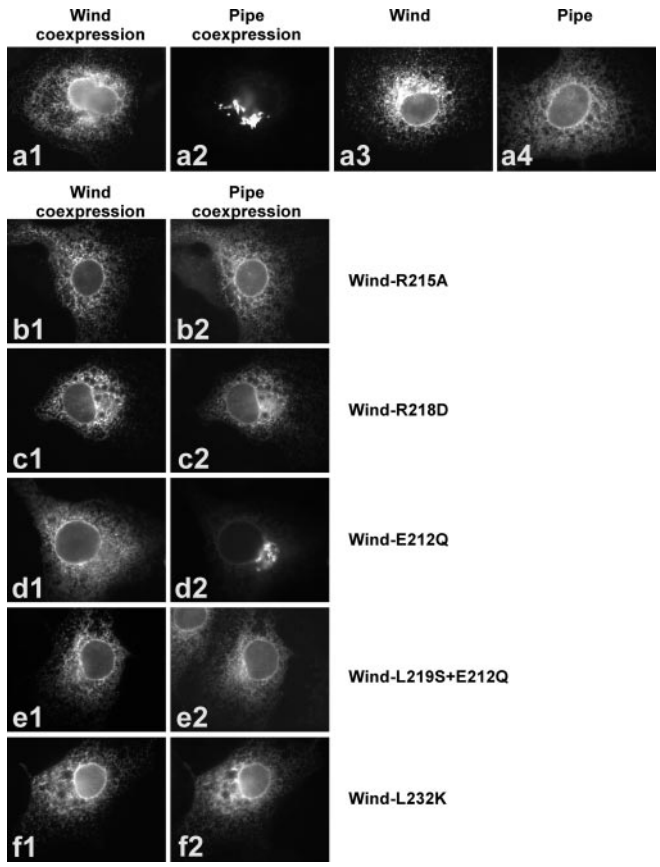

FIG. 8. **D-domain mutants affect Pipe processing.** In Vero cells expressing Pipe-GFP and the Wind E212Q mutant (*d1* and *d2*) Pipe transport is normal, similar to cells expressing Pipe-GFP and wild-type Wind (*a1* and *a2*). In contrast, the double mutant L219S/E212Q (*e1* and *e2*) efficiently inhibits Pipe processing, similar to the R215A (*b1* and *b2*), R218D (*c1* and *c2*), and L232K (*f1* and *f2*) mutants. Both Wind (*a3*) and Pipe-GFP (*a4*) are normally expressed and retained in Vero ER when expressed alone.

D31N mutation significantly impairs dimer formation *in vitro*, with most Wind present as monomer, but that this protein still supports Pipe processing *in vivo* (3). We wanted to know whether the ability of D31N to mediate Pipe processing was due to residual Wind dimer still being formed, or whether dimerized Wind was not important for processing at all.

Using an *in vitro* cross-linking approach, we found that D31N, when expressed in COS cells, still dimerizes significantly (Fig. 3, *panels a* and *g*). Furthermore, the purified, recombinant protein, although mainly monomeric, is unstable and aggregates with time (data not shown). We therefore chose to devise different mutants that produced monomeric Wind.

Two of these mutations, V28D and V28Y, targeted a semi-conserved residue at the heart of the dimer interface. Both mutants completely prevent dimerization *in vitro* and *in vivo* (data not shown) and cannot process Pipe. However, the proteins show a significant tendency to aggregate *in vivo*. This made it difficult to evaluate the results as being due to lack of dimerization, because one could argue that aggregation might sequester the protein away from the substrate. We therefore targeted another residue, Arg^{41}. Arg^{41}, which is in the turn between α1 and β2 on the opposite face of the dimer and at the edge of the dimerization surface, contributes significantly to dimer stability with hydrophobic interactions along its side chain. Although R41S alone cannot prevent dimerization of Wind (Fig. 3, *panel f*) and did not prevent Pipe processing (Fig. 9), the double mutant D31N/R41S eliminated dimerization *in vivo* (Fig. 3, *panel h*) and could not process Pipe, although the mutant was highly expressed (Fig. 9). Importantly, aggregation was significantly reduced compared with V28D and V28Y. Furthermore, the monomer of the Wind V28D mutant could be stabilized after incorporation of the R41S mutation (V28D/R41S) (Fig. 3, *panels i–j*), yet it still failed to process Pipe (data not shown). Taken together these results provide conclusive evidence that Wind dimer formation is required for efficient Pipe processing.

In our *in vivo* competition experiments, expression of the Wind D31N/R41S monomer causes a slight (20%) reduction in Pipe processing. This effect might be accounted for by the observed binding to the D-domain alone (as indicated in experiments using ss-D*, see Fig. 6). On the other hand, if any binding to the monomer did indeed occur via the b-domain, one might expect that insertion of the Y55K mutation into the monomeric Wind protein (triple mutant Y55K/D31N/R41S) would result in stronger binding in analogy to the dimeric Y55K protein, and either lead to degradation as observed for the Y55K dimer and Pipe, or to inhibition of processing by WT Wind in the stably transfected Vero system. In fact, neither effect is observed (Figs. 6 and 9) indicating that (*a*) the monomer is unlikely to bind strongly via the b-domain, (*b*) the Y55K dominant negative phenotype requires dimer formation, and (*c*) significant substrate binding to the b-domain requires Wind dimerization.

DISCUSSION

Wind is a PDI-related protein, from *D. melanogaster* that belongs to the PDI-D subgroup, in which it is further classified as a PDI-Dβ protein (D-domain-containing *PDI*-related protein with a *b*-type thioredoxin domain) (1). Here, we identify a putative substrate binding site in the Wind b-domain. The site is composed principally of a shallow pocket around Asp^{50}, with some localized hydrophobic character, and an aromatic tyrosine cluster (Fig. 10), including Tyr^{53} and Tyr^{55}, both of which occur in the turn before α2 (Fig. 4). Interestingly, this location corresponds to positions occupied by conserved residues in the a- and a′-domains of PDI-related proteins (WCGHC). Although Wind has a unique loop between β3 and α3 (the PDI-Dβ loop),

which contains the third member of the tyrosine cluster, neither this residue nor others within the loop are essential for Pipe processing, although the loop is close enough to the binding site that mutations within it could impair Wind activity significantly. Insertions of varying lengths do occur at this position in other thioredoxin fold proteins, such as in bacterial DsbA (16) and glutathione peroxidase (15). For DsbA, it is has been suggested that the inserted domain plays a role in substrate recognition or binding (14). Thus it may be that the PDI-Dβ loop is required for substrate specificity or even for some substrate binding, but direct interaction with residues within it is not required for Pipe processing. Mutation of either Tyr^{53} or Tyr^{55} or of residues within the PDI-Dβ loop (Y86Q or K84D) results in a stabilized interaction with Pipe. This effect, however, is unlikely to be mediated by local structural changes in the thioredoxin fold (3). Indeed, for the Y53S and Y53F mutants, recently determined crystal structures indicate that the exchanges neither perturb the thioredoxin fold nor impair dimer formation (Fig. 4).[3] Both Y53S and K84D mutants seem to stabilize the interaction of Wind with Pipe to such an extent that both proteins are eventually degraded. The requirement of the $Tyr^{53/55}$ pair is primarily related to their aromatic/hydrophobic nature, because both residues can be functionally replaced by phenylalanines.

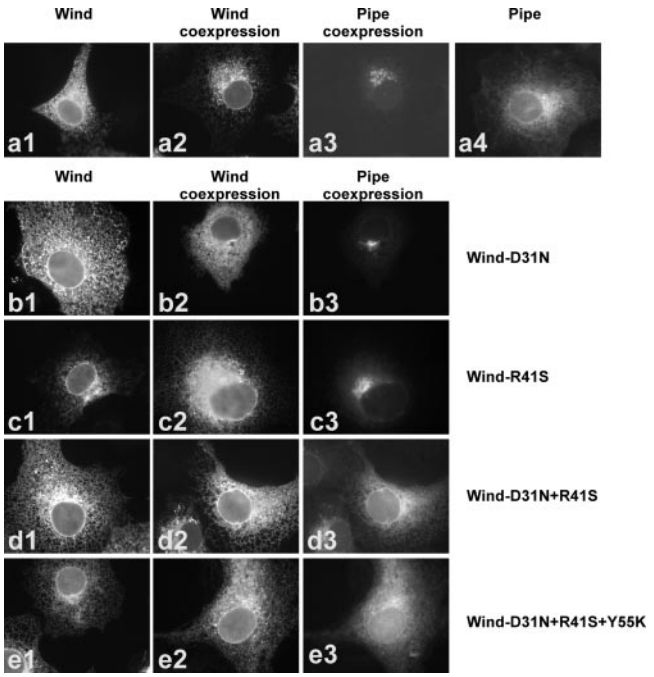

FIG. 9. **Dimeric Wind is required for Pipe processing in COS cells.** Asp^{31} and Arg^{41} localize to the top and bottom surfaces, respectively, of the Wind dimer. Mutation of one of these residues (D31N or R41S) does not significantly impede Pipe ER export when compared with WT Wind (*a3*, *b3*, and *c3*). However, the D31N/R41S double mutant no longer supports productive Pipe processing, resulting in the ER accumulation of Pipe-GFP. In contrast to Wind Y55K (see Fig. 5), levels of the triple mutant D31N/R41S/Y55K, which likewise does not support Pipe processing (*e3*), do not decrease during co-expression with Pipe (*e2*), indicating that the monomeric protein does not interact stably with Pipe. All mutants were expressed alone and with Pipe-GFP at normal levels (columns *a1–e1* and *a2–e2*, respectively).

The central role of the candidate peptide binding surface is supported by further data. When the N terminus of Wind, which is located within the dimer cleft, is extended by 14 residues, but not by 4 or 2 residues, Pipe processing in COS cells is significantly reduced, presumably by obstruction of access by bulky polypeptides to the tyrosine clusters around the dimer cleft. Peptide binding to denatured protein *in vitro*, however, is not affected, as might be expected if access to the dimer cleft itself is not necessary.

A second site in Wind required for Pipe processing seems to be present in the D-domain. Here, three residues (Arg^{215}, Arg^{218}, and Leu^{232}) form a surface of ~55 $Å^2$ between helices α8 and α9 on the same face of Wind as the tyrosine cluster of the b-domain (Fig. 10). Mutagenesis of any of these residues severely impairs Pipe transport to the Golgi. Two additional, nearby residues (Glu^{212} and Leu^{219}) may also be involved. The D-domain may bind independently of the b-domain to substrate *in vivo*, and it is essential, but not sufficient, for Pipe processing. This is the first tentative function to be assigned to the D-domain in higher eukaryotes. Because the residues studied here are highly conserved in most PDI-D proteins, and because the D-domain of mouse ERp29 can functionally replace the D-domain of Wind in Pipe processing, it is possible that substrate binding is a common feature of all members of this subfamily. It is of note that, although the b- and D-domains of Wind are connected by a short, flexible linker with two conserved glycines, neither these glycines nor other conserved residues are essential for Pipe processing.[4]

[4] K. Barnewitz, C. Guo, M. Sevvana, Q. Ma, G. M. Sheldrick, H.-D. Söling, and D. M. Ferrari, unpublished data.

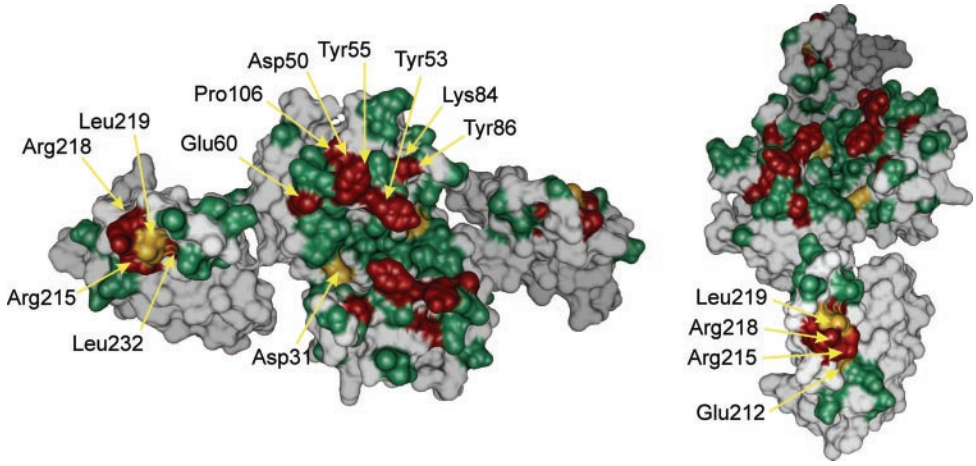

FIG. 10. **Mutations affecting Pipe processing map to two regions of the Wind protein.** Within both the b- and the D-domains, mutations that affect Pipe processing (*red*, labeled and indicated by *yellow arrows*) map to distinct, independent surfaces. Residues that have no effect when mutated alone, but that disrupt Pipe transport when combined with a second mutation are shown in *yellow*. Residues that when mutated have no adverse effect on Pipe export are shown in *green*. The dimeric molecule is shown in two different orientations. Arg^{41}, on the bottom face of the b-domain, is not visible here. This figure was produced with Chimera (available at www.cgl.ucsf.edu/chimera).

Wind dimerization creates an acidic cleft running immediately below the Tyr^{53}/Tyr^{55} couple. This cleft, although large enough to partially accommodate an extended peptide, is not essential for Pipe processing, but it may be used by other substrates. Wind dimerization is, however, essential for activity and may be required for substrate binding to the b-domain. Double mutants that stabilize the monomeric form of Wind, D31N/R41S and V28D/R41S, do not form dimers *in vivo* and cannot process Pipe. None of these residues are near the putative peptide binding sites of Wind, and neither D31N nor R41S alone show impaired Pipe processing activity. Furthermore, inclusion of the Y55K mutation into monomeric Wind (D31N/R41S) does not lead to significantly enhanced substrate binding in comparison to Y55K alone. A requirement for dimerization or for the participation of two or more, covalently linked thioredoxin domains in chaperone/redox activity has also been noted for bacterial DsbC and PDI (7, 17, 18).

Wind binds directly to multiple Pipe sequences *in vitro*, with a preference for sequences with two aromatic (Tyr or Phe) residues, but with no requirement for further conserved character in the peptides. The Wind Y55K mutant increases binding affinity, indicating binding affinities in the order FY > FF > YF > YXY (or YL) for peptides that are also recognized by wild-type Wind.

A putative peptide binding site, centered around a hydrophobic pocket containing the residues Leu^{242}, Leu^{244}, Phe^{258}, and Ile^{272} has recently been described for the b′-domain of human PDI (19). Mutation of these residues led to loss of binding to a synthetic substrate (Δ-somatostatin), with the greatest effect observed for the I272W mutant. Using the data the authors provide (19), Leu^{242} and Leu^{244} correspond to Lys^{48} and Asp^{50} in Wind. Both these residues do occur in a shallow pocket on the surface of Wind, flanked by Pro^{106} and Tyr^{55}, but here this pocket does not display overall strong hydrophobic character. We have shown that the D50A mutation does indeed lead to loss of Pipe processing, although a role for Lys^{48} was not investigated here as the residue shows very little surface exposure. Similarly, Phe^{258} and Ile^{272} in the b′-domain of PDI correspond to Phe^{62} and Thr^{80} in Wind. Both residues are completely buried near the Asp^{50} pocket, Thr^{80} being somewhat accessible from the dimer cleft. In Wind, the roles of the residues seems only structural, and neither of them is likely to be involved in substrate binding, indicating that further work may be necessary to verify the results from the PDI study.

In Wind, the other critical residues mentioned here would correspond to Ser^{247} (Wind Tyr^{53}) and Ser^{249} or Tyr^{251} (Wind Tyr^{55}) of the PDI b′-domain, whereas one of the PDI residues Ser^{276}, Asp^{277}, or His^{278} would correspond to Wind Tyr^{86}. Here, the possible conservation of Tyr^{55} is noteworthy, as is our finding that the Y53S mutation increases substrate binding affinity. Apart from PDI Ser^{249}, mutants of which had no effect on substrate binding (19), no work on these residues has been reported.

For PDIp, it has been shown that the protein binds peptides that contain a single Tyr or Trp residue, with the exception of peptides with an adjacent, negative charge (20, 21). In the case of PDI, substrate specificity has yet to be determined. From our results it is tempting to speculate that the major peptide binding sites in PDI proteins may be localized to regions of the b-domains corresponding to both the surface around the active site CGHC in the redox active a-domains, as well as the hydrophobic (PDI) or somewhat hydrophilic (Wind) pocket around residues corresponding to Wind Asp^{50}. Our data indicate that non-covalent peptide binding to PDI proteins indeed may require as little as one or two exposed aromatic/hydrophobic residues in the substrate.

Obviously, even such a small binding site offers specificity in substrate selection: whereas PDIp shows preference for a single Tyr or Trp residue, Wind has a predilection for two consecutive Phe or Tyr residues. Such small changes in substrate specificity may explain the necessity for the plethora of PDI-related proteins in the lumen of the ER. Furthermore, the minimal size of the substrate recognition motifs suggests that a majority of ER-resident or -secreted protein is likely to contain multiple copies of one or more of these motifs and may require the chaperone services of more than one of the PDI proteins to attain their native/secretion competent state. This would explain the relative abundance of several of the PDI proteins, which can be found at near-millimolar concentrations (22) in some tissues.

Acknowledgment—We thank R. Jahn for critical reading of the manuscript.

REFERENCES

1. Ferrari, D. M., and Söling, H. D. (1999) *Biochem. J.* **339,** 1–10
2. Freedman, R. B., Klappa, P., and Ruddock, L. W. (2002) *EMBO Rep.* **3,** 136–140
3. Ma, Q., Guo, C., Barnewitz, K., Sheldrick, G. M., Söling, H.-D., Usón, I., and Ferrari, D. M. (2003) *J. Biol. Chem.* **278,** 44600–44607
4. Hoshijima, K., Metherall, J. E., and Grunwald, D. J. (2002) *Genes Dev.* **16,** 2518–2529
5. Kemmink, J., Darby, N. J., Dijkstra, K., Nilges, M., and Creighton, T. E. (1996) *Biochemistry* **35,** 7684–7691
6. Kemmink, J., Dijkstra, K., Mariani, M., Scheek, R. M., Penka, E., Nilges, M., and Darby, N. J. (1999) *J. Biomol. NMR* **13,** 357–368
7. Klappa, P., Ruddock, L. W., Darby, N. J., and Freedman, R. B. (1998) *EMBO J.* **17,** 927–935
8. Sen, J., Goltz, J. S., Konsolaki, M., Schupbach, T., and Stein, D. (2000) *Development* **127,** 5541–5550
9. Monnat, J., Neuhaus, E. M., Pop, M. S., Ferrari, D. M., Kramer, B., and Soldati, T. (2000) *Mol. Biol. Cell* **11,** 3469–3484
10. Rudiger, S., Germeroth, L., Schneider-Mergener, J., and Bukau, B. (1997) *EMBO J.* **16,** 1501–1507
11. Hoff, K. G., Ta, D. T., Tapley, T. L., Silberg, J. J., and Vickery, L. E. (2002) *J. Biol. Chem.* **277,** 27353–27359
12. Nordstrand, K., Aslund, F., Holmgren, A., Otting, G., and Berndt, K. D. (1999) *J. Mol. Biol.* **286,** 541–552
13. Liepinsh, E., Baryshev, M., Sharipo, A., Ingelman-Sundberg, M., Otting, G., and Mkrtchian, S. (2001) *Structure* **9,** 457–471
14. Guddat, L. W., Bardwell, J. C., and Martin, J. L. (1998) *Structure* **6,** 757–767
15. Epp, O., Ladenstein, R., and Wendel, A. (1983) *Eur. J. Biochem.* **133,** 51–69
16. Martin, J. L., Bardwell, J. C., and Kurijan, J. (1993) *Nature* **365,** 464–468
17. Zhao, Z., Peng, Y., Hao, S.-f., Zeng, Z.-h., and Wang, C.-c. (2003) *J. Biol. Chem.* **278,** 43292–43298
18. Sun, X.-x., and Wang, C.-c. (2000) *J. Biol. Chem.* **275,** 22743–22749
19. Pirneskoski, A., Klappa, P., Lobell, M., Williamson, R. A., Byrne, L., Alanen, H. I., Salo, K. E. H., Kivirikko, K. I., Freedman, R. B., and Ruddock, L. W. (2004) *J. Biol. Chem.* **279,** 10374–10381
20. Ruddock, L. W., Freedman, R. B., and Klappa, P. (2000) *Prot. Sci.* **9,** 758–764
21. Klappa, P., Freedman, R. B., Langenbuch, M., Lan, M. S., Robinson, G. K., and Ruddock, L. W. (2001) *Biochem. J.* **354,** 553–559
22. Freedman, R. B., Hirst, T. R., and Tuite, M. F. (1994) *Trends Biochem. Sci.* **19,** 331–336